Enhancement of a Lewis Acid−Base Interaction via Solvation: Ammonia Molecules and the Benzene Radical Cation

Chi-Tung Chiang,[†] Marek Freindorf,[‡] Thomas Furlani,[‡] Robert L. DeLeon,[†] John P. Richard,[†] and James F. Garvey*[,†]

Department of Chemistry, University at Buffalo, State University of New York at Buffalo, Buffalo, New York 14260-3000, and Center for Computational Research, University at Buffalo, State University of New York at Buffalo, Buffalo, New York

Received: February 16, 2007; In Final Form: April 20, 2007

The interaction between ammonia and the benzene radical cation has been investigated by gas-phase studies of mass selected ion clusters $\{C_6H_6\text{-}(NH_3)_{n=0-8}\}^+$ via tandem quadrupole mass spectrometry and through calculations. Experiments show a special stability for the cluster ion that contains four ammonias: $\{C_6H_6\text{-}(NH_3)_4\}^+$. Calculations provide evidence that the first ammonia forms a weak dative bond to the cyclohexadienyl radical cation, $\{C_6H_6{-}NH_3\}^+$, where there is a transfer of electrons from ammonia to benzene. Additional solvating ammonia molecules form stabilizing hydrogen bonds to the ring-bound ammonia $\{C_6H_6{-}NH_3\}^+\cdot(NH_3)_n$, which cause cooperative changes in the structure of the cluster complex. Free ammonia is a weak hydrogen bond donor, but electron transfer from NH_3 to the benzene ring that strengthens the dative bond will increase the hydrogen acidity and the strength of the cluster hydrogen bonds to the added ammonia. A progressive "tightening" of this dative bond is observed upon addition of the first, second, and third ammonia to give a cluster stabilized by three $N{-}^+H\cdot N$ hydrogen bonds. This shows that the energetic cost of tightening the dative bond is recovered with dividends in the formation of stable cluster hydrogen bonds.

Introduction

Molecular beam studies of gas-phase ions, supported by calculations, is an attractive method to study the details of molecular interactions and chemical reactivity. This present study explores the interaction between an electron deficient benzene radical cation and neutral ammonia molecules, as an example of how solvation can modify the standard Lewis acid−base interaction.

Both simple carbocations and related cation radicals, such as the benzene radical cation, may be generated in the gas phase, but there have been few studies of nucleophile addition to these electrophiles. The highly electron-deficient benzene cation **1** is far too unstable to exist in nucleophilic solvents,[1−3] but this cation may be generated in the gas phase[4] where it undergoes "barrierless" reactions with added nucleophiles such as water (Scheme 1),[2] and even nitrogen-containing molecules.[2,3] There is a strong driving force for addition of a hydrogen atom to the benzene cation to form the radical cation **2**.[4] However, the chemistry associated with nucleophile addition to **2** has not been investigated in detail. There have been few experimental or theoretical studies of radical cation−nucleophile combination reactions.[5] The benzene radical cation is expected to be less eletrophilic than the parent benzene cation, because the product of nucleophile addition is itself an unstable radical or radical cation (Scheme 1). For example, the addition of water to the benzene radical cation (C···O interaction) is predicted by calculations to be thermodynamically unfavorable.[6]

The solvation and microsolvation of aliphatic and aromatic carbocations by polar molecules has attracted attention in recent years due to the importance of these interactions in many chemical, biological, and physical phenomena.[7−18] In particular, small clusters of molecules provide a unique environment for detailed studies of the interactions between an aromatic radical cation and a polar "solvent". The gas-phase aromatic radical, such as the benzene radical cation can react with nucleophilic neutrals, such as ammonia, to produce the gas-phase analog of a solution-based nucleophilic substitution (S_N2) reaction. See (Scheme 2).[10,14]

SCHEME 1

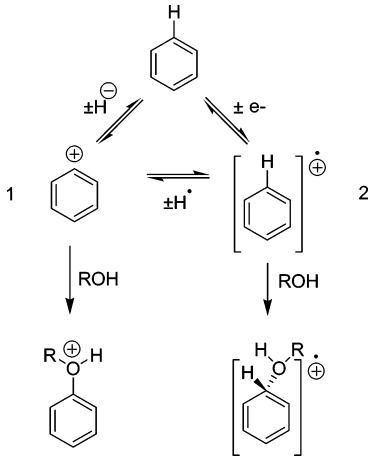

A structure for the cluster formed between a single ammonia and the benzene radical cation has been proposed by Tachikawa on the basis of the results of density functional theory (DFT) calculations at the B3LYP/6-311G(d,p) level.[19] The calculations are consistent with the formation of a long, weak, valence bond between the ammonia nitrogen and a benzene carbon with a

* Corresponding author. E-mail: garvey@buffalo.edu.
[†] Department of Chemistry.
[‡] Center for Computational Research.

10.1021/jp071349c CCC: $37.00
Published on Web 06/15/2007

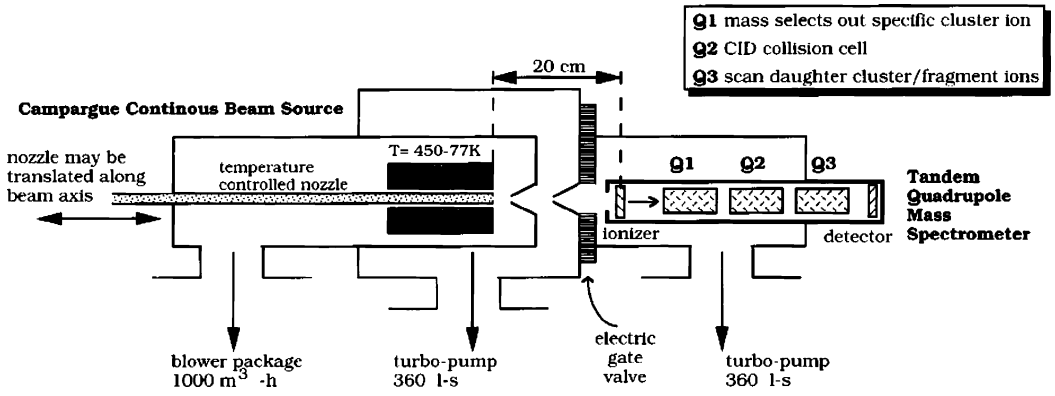

Figure 1. Schematic drawing of the apparatus.

SCHEME 2

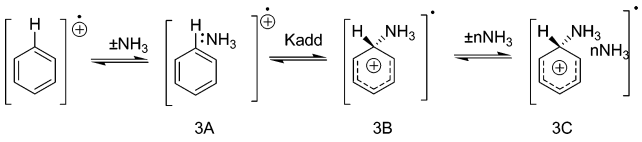

C−N bond distance of 1.628 Å (**3B**). This calculated structure was then later confirmed by Mikami and co-workers by employing infrared and electronic spectroscopy as well as calculations at the B3LYP/6-311G++(d,p) level of theory.[20] Both experiments and calculations are consistent with the conclusion that the species where ammonia shows a largely electrostatic interaction with the benzene radical cation, **3A**, and the covalent species **3B** are close in energy, presumably because the stabilization gained from formation of the covalent C−N bond is roughly balanced by the destabilization associated with the loss of aromaticity on formation of the "cyclohexadienyl" ring. These experimental and computational studies have been limited to the 1:1 benzene−ammonia cluster. The addition of further ammonia molecules (**3C**), is expected to stabilize the covalent adduct **3B** relative to **3A**. This is due to a greater concentration of charge at the ammonia hydrogen at **3B** favoring formation of stabilizing hydrogen bonds to ammonia. We are interested in quantifying the stabilization of this covalent C−N bond due to clustering with added ammonia and in characterizing the changes in the length of the bond that occur with the formation of additional hydrogen bonds to the ring-bound ammonia.

We report here the energetic and structural properties of benzene−ammonia cluster ions $\{C_6H_6(NH_3)_n\}^+$ determined by Campargue-type molecular beam and tandem quadrupole mass spectrometry. The relative stabilities of these ions were determined from the conventional mass spectrum. Collision induced dissociation (CID) of mass selected cluster ions was performed to characterize the structure of these clusters and to locate the positive charge within the cluster. The relative energies of these clusters were obtained from calculations using the density functional theory (DFT) at the B3LYP/6-311+G(d,p) level.

Experimental Section

A schematic of the molecular beam apparatus employed for these experiments is shown in Figure 1. It consists of a Campargue-type continuous molecular beam source coupled to a triple quadrupole mass spectrometer (Extrel C-50).[21,22] The benzene−ammonia mixture was introduced by passing gaseous ammonia through a bubbler containing the liquid benzene reagent. A neutral cluster beam was generated by the adiabatic expansion of the mixed vapor at a stagnation pressure of 1.5 atm supersonically through a 250 μm nozzle at a nozzle temperature of 291 K. Before entering the tandem mass spectrometer chamber, the neutral cluster beam was collimated by two conical nickel skimmers. A small fraction of the neutral clusters was ionized by electron impact (EI) ionization with an electron energy of 70.0 eV and an emission current of 3.0 mA. The ionized clusters are then focused and guided into the first quadrupole (Q1) of the triple quadrupole mass spectrometer by employing collinear ion optics.

The first (Q1) and third (Q3) quadrupoles both have a nominal mass range of 1200 amu and can be operated in either "rf" or "dc" mode. The second quadrupole (Q2) is always at "rf-only" mode to guide the cluster ions to (Q3) and contains a gas collision cell for CID experiments. In this study, the collision gas is argon, and the collision cell pressure was maintained at $(9.0 \pm 1.0) \times 10^{-4}$ Torr for all CID experiments. The background pressure in the mass spectrometer chamber was approximately $(4.0 \pm 1.0) \times 10^{-6}$ Torr with the beam on and collision gas in the collision chamber, and $(2.0 \pm 1.0) \times 10^{-7}$ Torr with no collision gas in the collision cell. Two scan modes were employed in this experiment. The first was a conventional mass scan mode by operating (Q1) and (Q2) in "rf-only" mode, and scanning the third quadrupole (Q3). For CID experiments, (Q1) was used to mass-select a particular cluster ion, (Q2) was run in "rf-only" mode with argon in the collision cell, and (Q3) was scanned to observe the product ions exiting the collision cell. Observed in such a scan is the mass selected parent ion as well as any daughter ions resulting from fragmentation and/or chemical reaction in the collision cell. Ions were detected by an off-axis channeltron device and the output signal was then passed through a 1.5 kHz low pass filter. The final mass spectra were averaged and recorded by a LeCroy 9310A digital oscilloscope. A collision energy of 10 eV, in the lab frame of reference, was used for all experiments, and is defined as the potential difference between the ionization region and the (Q2) ion optics. Reagent grade benzene was obtained from Merck, anhydrous ammonia (>99.99%) was from Matheson, and argon (>99.9%) was from Irish Welding Supply.

Calculational Details

The calculations were performed at the DFT level of theory using the B3LYP[23,24] hybrid functional and utilizing the 6-311+G(d,p) basis set[25] (triple-ζ valence quality with diffuse and polarization functions). This level of theory has been proven in the literature to be a precise computational approach in calculations involving hydrogen bonds[26] and is an excellent compromise between computational accuracy and computational efficiency. We calculated optimal geometries and electrostatic potentials of clusters built of ammonia molecules and the

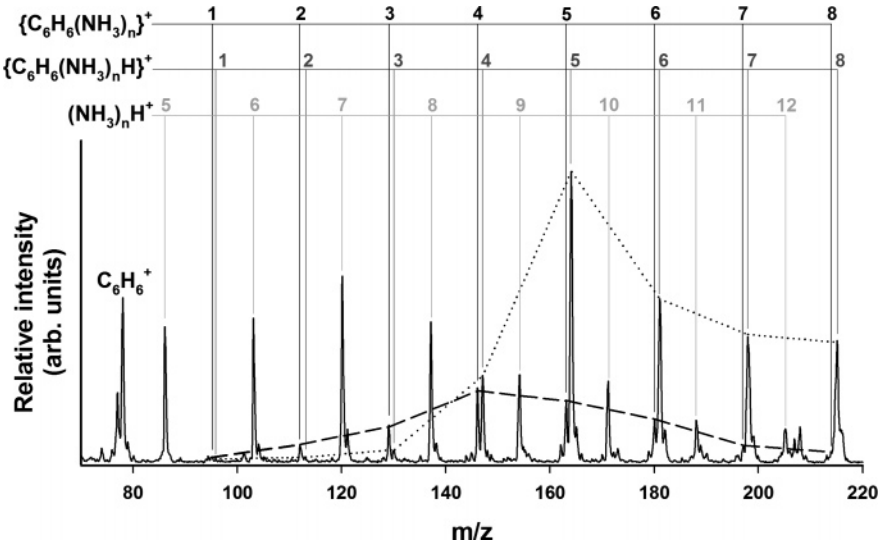

Figure 2. Q3 survey mass spectrum of ion clusters generated from pure benzene vapor seeded in anhydrous ammonia via electron impact ionization. The dotted line connects the peaks of the protonated series $\{C_6H_6(NH_3)_nH\}^+$, and the dashed line connects the peaks of the unprotonated series $\{C_6H_6(NH_3)_n\}^+$.

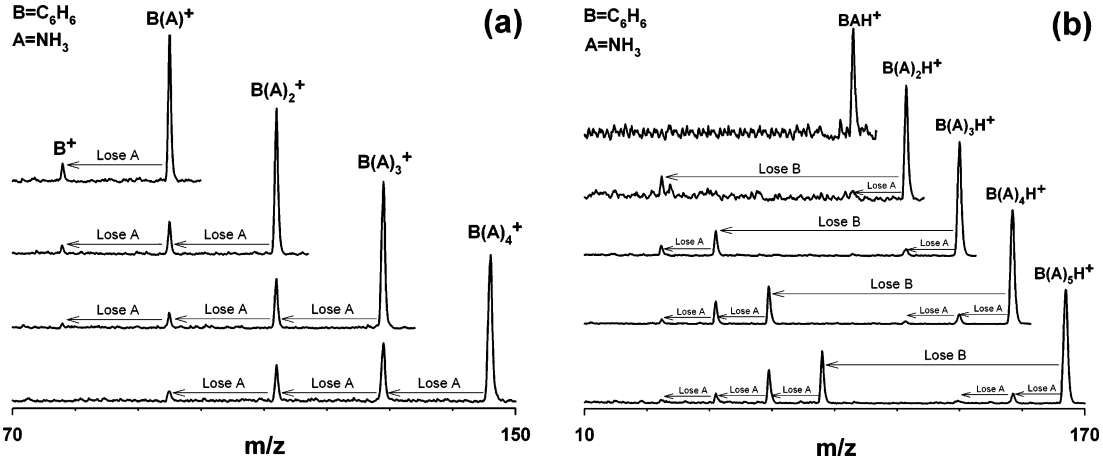

Figure 3. CID spectra of (a) $\{C_6H_6(NH_3)_n\}^+$, $n = 1-4$, and (b) $\{C_6H_6(NH_3)_nH\}^+$, $n = 1-5$.

benzene radical cation, without any constraint in the gas phase, allowing C_1 symmetry for all calculated molecular systems. The cluster bonding energy was calculated as the difference between the calculated energy for the cluster and the sum of the calculated energies of the separated monomers. Basis set superposition error correction was not employed in our calculations of bonding energy, because the quality of the basis set used in our calculations does not require it (see Supporting Information Table S1). Both the Mulliken charge population and the natural bond orbital (NBO) charge analysis were calculated to characterize the charge distribution. The calculations were performed for a doublet electronic state, which is the ground electronic state of the cation system, and for a singlet electronic state of the neutral system and the protonated benzene−ammonia cluster. The calculations have been performed using the Q-Chem program.[27] To illustrate the electronic density distribution, we have also calculated the electrostatic potential mapped on the electronic density by employing the Spartan program at the B3LYP/6-31G(d,p) level of theory.

Results and Discussion

Conventional Mass Spectrometry. A conventional mass spectrum is shown in Figure 2 for benzene−ammonia cluster ions. A mass to charge ratio (m/z) range between 70 and 220 was scanned to observe the relative ion intensity of the benzene−ammonia cluster cations. Only singly charged clusters were observed in this spectrum; hence the m/z of each cluster will be referred to as its mass (in amu).

This spectrum is dominated by three cluster ion series: $(NH_3)_nH^+$, $\{C_6H_6(NH_3)_n\}^+$, and $\{C_6H_6(NH_3)_nH\}^+$, respectively. The protonated ammonia series of $(NH_3)_nH^+$, $n = 5-12$, is formed via exothermic proton-transfer reactions within neat ionized ammonia clusters. Two different series of benzene−ammonia clusters were observed. The first is $\{C_6H_6(NH_3)_n\}^+$, $n = 1-8$, which is the focus of this work. Generation of this type of cluster can be expressed as:

$$C_6H_6(NH_3)_{n+m} + e^- \rightarrow \{C_6H_6(NH_3)_{n+m}\}^+ + 2e^- \quad \text{Ionization (1)}$$

$$\{C_6H_6(NH_3)_{n+m}\}^+ \rightarrow \{C_6H_6(NH_3)_n\}^+ + mNH_3 \quad \text{Evaporation (2)}$$

The other series is the protonated benzene−ammonia cluster series $\{C_6H_6(NH_3)_nH\}^+$, $n = 1-8$. These clusters are formed by the interaction of a neat protonated ammonia cluster ion and a neutral benzene molecule. Clusters composed of more than

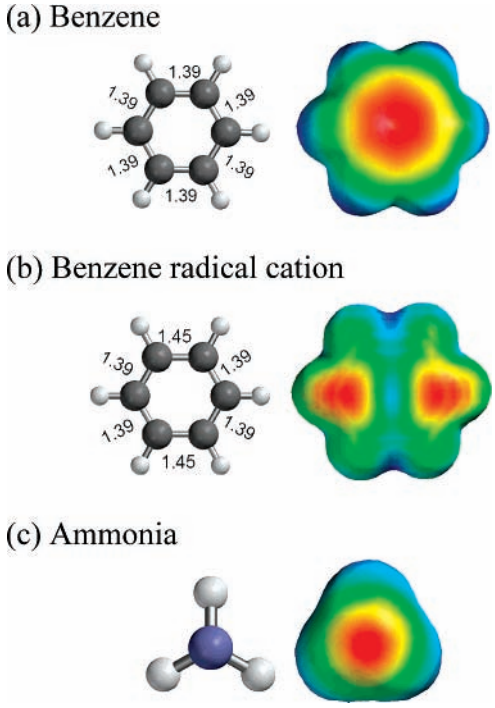

Figure 4. Optimized geometries and electrostatic potential for neutral benzene (a), the benzene radical cation (b), and neutral ammonia (c).

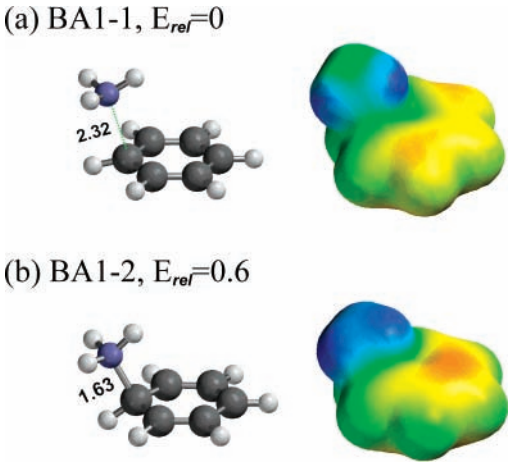

Figure 5. Optimized geometries and electrostatic potential of (a) BA1-1 and (b) BA1-2 isomers of $\{C_6H_6(NH_3)\}^+$.

one benzene are also seen in this mass spectrum, but their structures are not assigned in this paper. The relative ion intensity of these two series of clusters is indicated by the connected dashed line and dotted line, which highlights that there are two different size distributions and that the largest peak in each series is $\{C_6H_6(NH_3)_4\}^+$ and $\{C_6H_6(NH_3)_5H\}^+$, respectively. This also suggests that these two series of clusters have different structures and were formed by different mechanisms.

Collision Induced Dissociation Mass Spectra of $\{C_6H_6(NH_3)_n\}^+$ and $\{C_6H_6(NH_3)_nH\}^+$, $n = 1-4$. CID spectra were obtained for several cluster ions observed in the conventional mass spectrum. CID analysis has been an ideal method to elucidate the structures of parent cluster ions because the fragments or the loss of neutral molecules provides qualitative information about the intermolecular interaction within a cluster. Cluster ions of interest were first mass-selected by (Q1) and then guided through (Q2) containing a collision cell with argon gas. The fragmentation or reaction product ions exiting the collision cell were then mass-analyzed by (Q3). To easily visualize and compare the various reaction channels and fragments as a function as increasing cluster size, each spectrum in the same series of clusters is superimposed and offset. The CID spectra for the $\{C_6H_6(NH_3)_n\}^+$, $n = 1-4$, and $\{C_6H_6(NH_3)_nH\}^+$, $n = 1-5$, are shown in Figure 3. The CID results for these two series of benzene−ammonia clusters are in good agreement with the conventional mass spectrum in that the signal-to-noise ratio (S/N) of each CID spectrum is proportional to the ion abundance of the parent cluster ion.

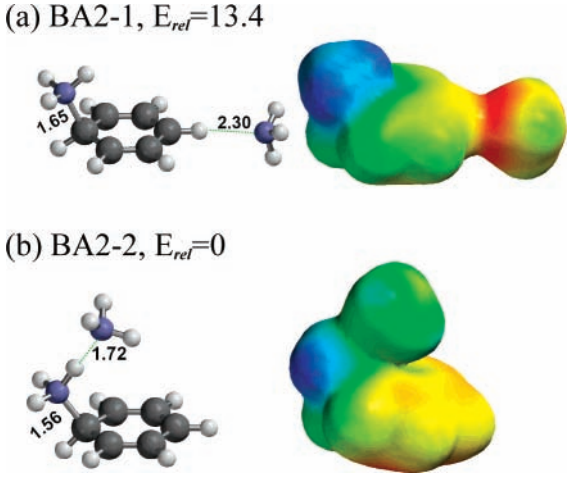

Figure 6. Optimized geometries and electrostatic potential of (a) BA2-1 and (b) BA2-2 isomers of $\{C_6H_6(NH_3)_2H\}^+$.

For the cluster series $\{C_6H_6(NH_3)_n\}^+$, two possible CID processes might be expected to occur:

$$\{C_6H_6(NH_3)_n\}^+ \rightarrow \{C_6H_6(NH_3)_{n-m}\}^+ + mNH_3 \quad (3)$$

$$\rightarrow \{C_6H_5{-}NH_3\}^+ - (NH_3)_{n-m-1} + mNH_3 + H \quad (4)$$

Reaction 3 represents the simple sequential evaporative loss of neutral ammonia molecules from the benzene−ammonia cluster ion, and reaction 4 is the S_N2 reaction product $\{C_6H_5{-}NH_3\}^+$ and its related clusters. In this experiment we observe only the evaporative loss of ammonia molecules. This suggests that the positive charge within the cluster is retained on the benzene moiety due to the substantially lower ionization potential (9.25 eV) of benzene compared to that of ammonia (10.16 eV).[28] The observation that reaction 4 does not occur at all, even in large clusters, strongly suggests that there is a large energy barrier for the substitution reaction.

For the cluster series $\{C_6H_6(NH_3)_nH\}^+$, two channels are observed:

$$\{C_6H_6(NH_3)_nH\}^+ \rightarrow (NH_3)_nH^+ + C_6H_6 \rightarrow (NH_3)_{n-m}H^+ + mNH_3 + C_6H_6 \quad (5)$$

$$\rightarrow \{C_6H_6(NH_3)_{n-m}H\}^+ + mNH_3 \rightarrow mNH_3 + (NH_3)_{n-m}H^+ + C_6H_6 \quad (6)$$

Based on the daughter ion intensity, reaction 5 is the main reaction channel indicating that in these protonated clusters, the benzene molecule is neutral. As a result, a neutral benzene or the neutral ammonias can both be evaporated from the cluster ion. Loss of the neutral benzene in both reaction channels indicates that the positive charge is localized on the protonated ammonia. This also indicates that the structures of protonated

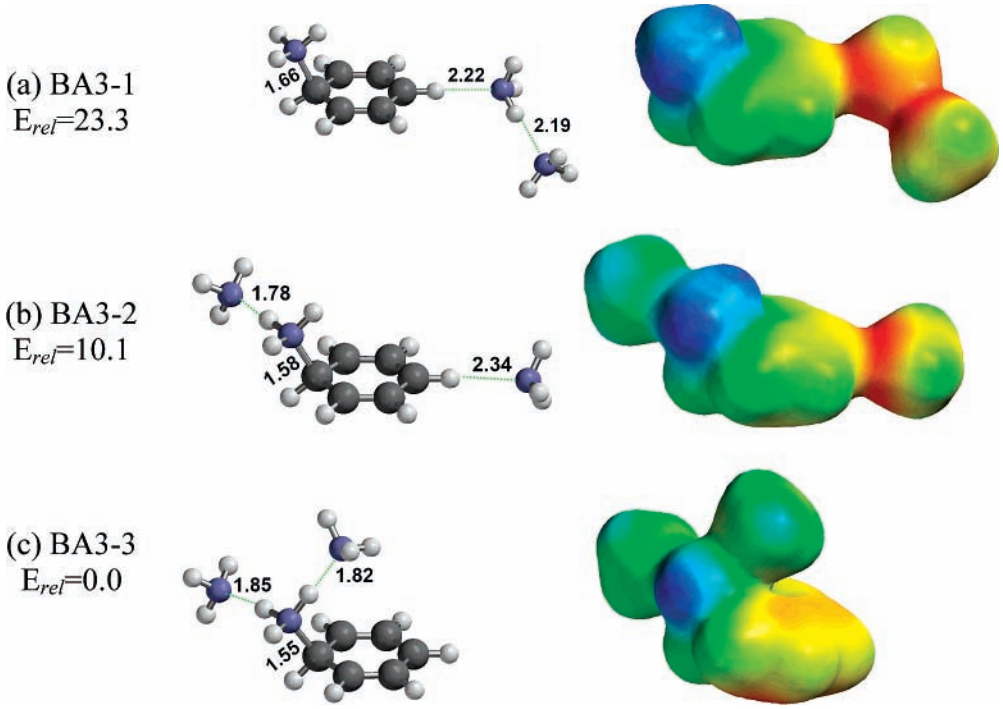

Figure 7. Optimized geometries and electrostatic potential of (a) BA3-1, (b) BA3-2, and (c) BA3-3 isomers of $\{C_6H_6(NH_3)_3\}^+$.

benzene−ammonia cluster ions are entirely different from unprotonated benzene−ammonia cluster ions.

Cluster Structures and Electrostatic Potential. We first calculated the neutral benzene and the benzene radical cation to compare a difference in their structures and electrostatic potential upon ionization, as a benchmark for further calculations. For the $\{C_6H_6(NH_3)\}^+$ cluster, we calculated a structure similar to the one previously reported by Mikami.[20] For the $\{C_6H_6(NH_3)_{n=2-4}\}^+$ cluster ions, structures were calculated on the basis of the "cyclohexadienyl" type of the benzene−ammonia cation to better understand the role of the ammonia solvent molecules within the cluster structure. The optimized structure of each isomer was obtained to compare their relative stability and binding features. The electrostatic potential shows the distribution of the electronic density within each cluster structure. Figures 4−9 show optimized geometries and corresponding electrostatic potentials for the cluster ions in the series $\{C_6H_6(NH_3)_{n=1-4}\}^+$. We also calculated the optimized geometry of $\{C_6H_6(NH_3)_5H\}^+$ to illustrate the different binding features between protonated and unprotonated benzene−ammonia clusters. The relative bonding energies between various isomers and relevant intermolecular distances are labeled for comparison purposes. Bond lengths are expressed in angstroms. E_{rel} is the energy, in kcal mol^{-1}, relative to the most stable isomer. In Figures 4−9, a red color indicates electron rich areas, a blue color indicates electron poor areas, and green and yellow colors are intermediate.

C_6H_6, $C_6H_6^{+\bullet}$, and NH_3. Optimized structures and electrostatic potentials for the neutral benzene molecule (Figure 4a) and its radical cation (Figure 4b) both exhibit high symmetry. For the neutral benzene the electronic density is high on the center-of-mass of the benzene ring and low on the six hydrogen atoms. This is consistent with the result that the dipole of a polar molecule points toward the center-of-mass of benzene in the neutral cluster system.[19,29−30] However, in the case of the benzene radical cation (Figure 4b), its structure is distorted by the Jahn−Teller effect, in which electrons in a doubly degenerate molecular orbital interact with the nuclear coordinates.[31] In contrast, the electronic density is low in the central area and high on the opposite sides of the benzene ring. The electrostatic potential of the benzene radical cation clearly illustrates that the attractive dipole interaction of the neutral cluster would change to a repulsive one when an electron is removed from the benzene moiety. The optimized structure and electrostatic potential of the neutral ammonia molecule is shown in Figure 4c, indicating that the electron density is rich in the lone pair electron area and poor on the three hydrogen atoms. With these images of the electrostatic potential, it is easy to predict that the electron rich nitrogen will be attracted to the electron poor region on the benzene radical cation.

$\{C_6H_6(NH_3)\}^+$. For the $n = 1$ cluster, we calculated two isomers, labeled BA1-1 and BA1-2 (Figure 5), which are very similar to that calculated by Tachikawa and Mikami.[19,20] The C−N distance is 2.32 Å for BA1-1 and 1.63 Å for the isomer BA1-2. We also note that isomer BA1-1 is slightly more stable than isomer BA1-2 by 0.6 kcal mol^{-1}. Although the structure of the benzene−ammonia cation has been experimentally confirmed by infrared and electronic spectroscopy[20] to be BA1-2, the small calculated energy difference between the isomers suggests that both may play a role. Comparing their electrostatic potential with the neat benzene radical cation, we note, in both isomers, that the electronic density on the ammonia moiety has been transferred to the benzene ring. The C−N valence bond between the benzene radical cation and the ammonia is formed by the unpaired electron from the benzene and one electron from the ammonia lone pair; that is, the lone pair electrons of the ammonia partially donate electronic density from ammonia to the benzene radical cation. CID experiments on the $\{C_6H_6(NH_3)\}^+$ cluster provide strong evidence that the formation of this cluster by addition of ammonia to the benzene radical cation is a fully reversible process.

$\{C_6H_6(NH_3)_2\}^+$. Two isomers were calculated for the $n = 2$ cluster by placing the additional "solvent" ammonia either adjacent to the ammonia already bonded to the benzene or at the opposite (para) side of the ring, as shown in Figure 6. The calculation shows a very large energy difference between the

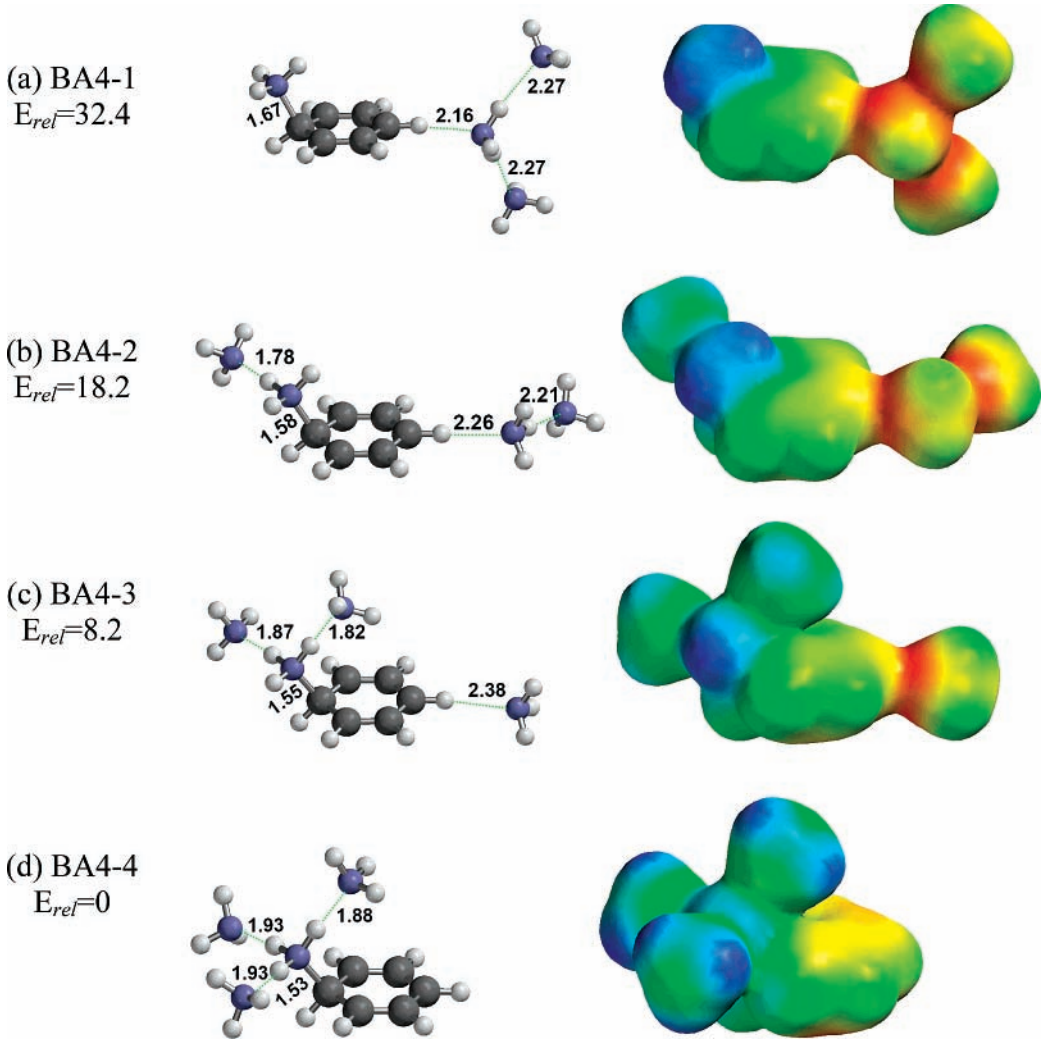

Figure 8. Optimized geometries and electrostatic potential of (a) BA4-1, (b) BA4-2, (c) BA4-3, and (d) BA4-4 isomers of $\{C_6H_6(NH_3)_4\}^+$.

two isomers in that isomer BA2-2 is more stable than isomer BA2-1 by 13.4 kcal mol^{-1}. The C−N length is also reduced in BA2-2 to 1.56 Å by the additional NH_3 hydrogen bonded to the ammonia, making it 0.07 Å shorter than in BA1-2. The addition of this second ammonia to the cluster causes an apparent strengthening of the dative C−N bond with the electronic density shifting to the benzene radical cation. As seen before, the only reaction channel observed in the CID spectrum of $\{C_6H_6(NH_3)_2\}^+$ is the evaporative loss of ammonia molecules, resulting in a lone benzene radical cation. Once again, as the "solvent" ammonia molecules evaporate, the electronic density is returned back to the ammonia.

$\{C_6H_6(NH_3)_3\}^+$. For the $n = 3$ cluster, as shown in Figure 7, we calculated three isomeric structures: BA3-1 has two ammonias para to each other and the third is hydrogen bonded to the non-ring-bonded ammonia, BA3-2 has two ammonias para to each other with the third ammonia hydrogen bonded to the ring-bound ammonia, and last, BA3-3 where the two additional ammonias are now both hydrogen bonded to the ring-bound ammonia. The most stable isomer is BA3-3 with a C−N distance of 1.55 Å. Again, it is very apparent that the stability of the cyclohexadienyl complex was further enhanced by the presence of the two additional "solvent" ammonia molecules. The energy difference between isomer BA3-1 and BA3-2 is 13.2 kcal mol^{-1} ,which we note is essentially the same difference as between BA2-1 and BA2-2. The energy difference between isomer BA3-2 and BA3-3 is 10.1 kcal mol^{-1}. The electrostatic potential of these three isomers is similar to that seen in Figure 6 for the $n = 2$ cluster, where there is a strengthening in the apparent dative bond interaction between the ammonia nitrogen and the benzene carbon. The CID result likewise shows a similar pattern with the $n = 2$ cluster in that the loss of ammonia monomers is the only reaction channel.

$\{C_6H_6(NH_3)_4\}^+$. In the conventional mass spectrum, Figure 2, this cluster ion was observed as the most stable cluster in the $\{C_6H_6^+(NH_3)_{n=1-8}\}$ series. The calculated structure reveals that the unique stability of this cluster is due to the three additional ammonia molecules that form three hydrogen bonds with the ring-bound ammonia moiety and further stabilize the cyclohexadienyl complex, as shown in Figure 8. Four isomers were calculated: BA4-1 has two ammonias para to each other and the two additional ammonias are both hydrogen bonded to the non-ring-bonded ammonia, BA4-2 has two ammonias para to each other with a single ammonia hydrogen bonded to the ring-bound ammonia and to the non-ring-bound ammonia, BA4-3 has two ammonias para to each other with two ammonias hydrogen bonded to the ring-bound ammonia, and last, BA4-4 has one ammonia ring bound and the other three are hydrogen bonded to it. The most stable isomer is BA4-4, where the C−N distance is 1.53 Å shorter than a regular C−C covalent bond (1.54 Å), but still longer than a regular C−N bond (1.43 Å).[32] This strongly suggests that the stability of the cyclohexadienyl complex is gradually enhanced by increasing the number of solvent ammonia molecules hydrogen bonded to the ring-bound

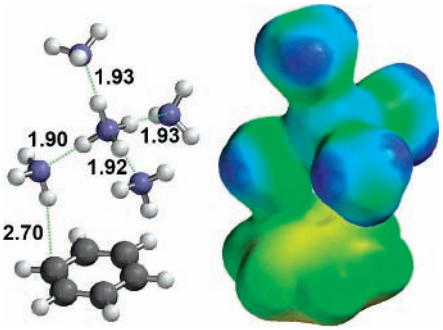

Figure 9. Optimized geometry and electrostatic potential of $\{C_6H_6(NH_3)_5H\}^+$.

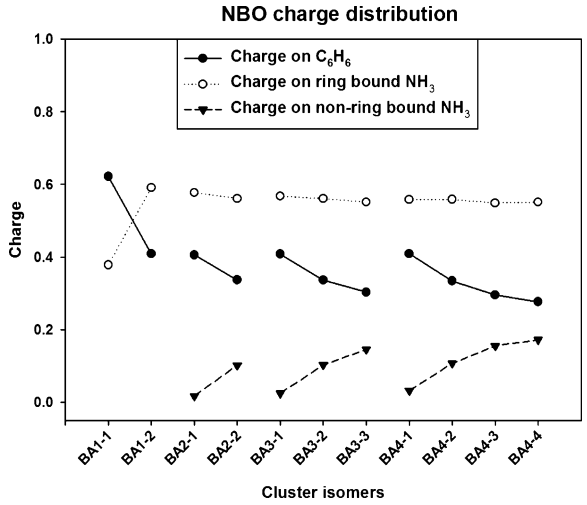

Figure 10. NBO charge distribution on C_6H_6, the ring-bound NH_3 and the non-ring-bound NH_3 for $\{C_6H_6(NH_3)_{n=1-4}\}^+$ as a function of the cluster isomer.

ammonia. The electrostatic potential again shows that electronic density from ammonia is transferred to the benzene moiety of the cyclohexadienyl complex, and the CID results show only the dissociation of ammonia monomers.

$\{C_6H_6(NH_3)_5H\}^+$. As seen in Figure 9, the protonated benzene−ammonia cluster demonstrates a different geometrical structure and a different electronic structure as compared to the unprotonated benzene−ammonia cluster series. The central NH_4^+ is completely solvated by forming four hydrogen bonds to four NH_3 monomers, which is nearly identical to the neat protonated ammonia cluster $(NH_3)_5H^+$ that is the "magic number" structure.[33] Benzene is neutral and bonded to the outside of the NH_4^+ solvation shell by weak van der Waals forces. This cluster structure is able to explain the experimental CID spectra for $\{C_6H_6(NH_3)_nH\}^+$ in that the loss of neutral benzene is the main reaction channel instead of losing ammonia.

Charge Distribution. As mentioned earlier, the formation of the $\{C_6H_6(NH_3)\}^+$ cluster is a fully reversible process. The distribution of the electronic density is considered to be a significant factor in determining the overall stability of the cluster ion. As singly charged clusters, the total charge population of each cluster is taken to be +1. Figure 10 shows the natural bond orbital (NBO) charge distribution. Approximately 40% of the charge is distributed on the ammonia moiety of isomer BA1-1 and increases to 60% on isomer BA1-2. For isomers $n = 2-4$, the charge remains near this 60% level on the ring-bound NH_3 with increasing electron withdrawal from the C_6H_6 ring by the solvating ammonias. The NBO charge distribution implies that more electronic density has been transferred to stabilize the cyclohexadienyl complex and enhance

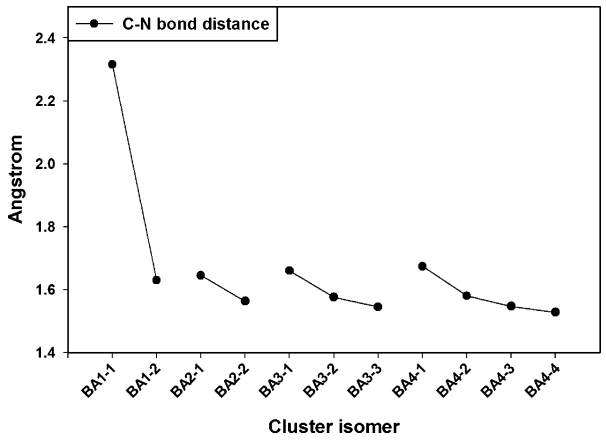

Figure 11. C−N bond distance between C_6H_6 and the ring-bound NH_3 for $\{C_6H_6(NH_3)_{n=1-4}\}^+$ as a function of the cluster isomer.

the C−N bond strength when the ring-bound NH_3 is hydrogen bonded to additional NH_3 molecules. Figure 11 shows how this bond distance contracts as additional ammonia molecules are added to the $\{C_6H_6(NH_3)\}^+$.

Discussion. This work shows that two types of cationic cluster ions between ammonia and benzene, that differ by 1 amu, can be prepared. The first type cluster forms by mixing the benzene radical cation and ammonia, and the second type forms by mixing neutral benzene, neutral ammonia, and the ammonium cation.

Ammonia shows nonbonding electronic interactions with the benzene radical cation **3A**, and there may be formal electron transfer from ammonia to the benzene ring to give a dative bond **3B**. There is little or no thermodynamic driving force to bond formation to ammonia ($K_{add} \approx 1$, Scheme 3), because the orbital for the electron-pair acceptor is already partly filled, and bond formation is accompanied by loss of a stabilizing cyclic array of 5π electrons.

The carbon-nitrogen bond in **3B** is long (1.63 Å, Scheme 3) and there will be an energetic price for its compression to a shorter length. The cost of compressing this bond from 1.63 Å at **3B** to 1.56 Å at **3C** is related to the increase in the strength of the −N−H•N− hydrogen bond that occurs as the dative bond is shortened and the cationic character at the hydrogen bond donor is increased. The bond shows a further decrease to 1.53 Å at **3D**, where there is now a maximum of three N−H•N− hydrogen bonds.

Note that there is little or no advantage to the formation of the isolated bond at **3B**, and yet the bond can be made to *appear* to be strong at **3D** by adding ammonia molecules that specifically stabilize the product by formation of hydrogen bonds that are stronger than those to the reactant complex. Cleavage of the dative C−N bond at **3D** to form the benzene radical cation and an ammonia cluster is unfavorable, not because there is effective covalent overlap between the bonding electrons, but because cleavage of this bond reduces the strength of the cluster ammonia hydrogen bonds.

It is interesting to show how the electronic properties of the C−N chemical bond change as additional ammonia molecules are added to make larger clusters. The charges, spin densities, and atomic populations have been calculated according to the natural bond orbital (NBO) analysis, using the B3LYP/6-311+G(d,p) level of theory. As indicated in Table 1, the bond length between the C and N atoms systematically decreases with an increasing number of ammonia molecules in the cluster. The biggest difference of this bond length (2.32 Å for cluster BA1-1 and 1.63 Å for cluster BA1-2) is observed for the two different

SCHEME 3

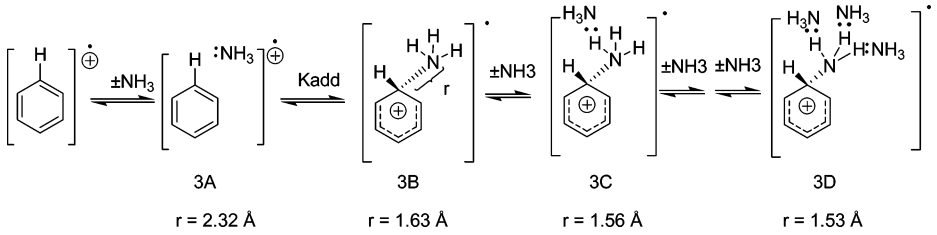

TABLE 1: Electronic Properties of the Interactive C and N Atoms of Selected Cluster Isomers[a]

		NBO charge (au)		NBO spin (au)		NBO population (au)			
cluster	C−N bond (Å)	C	N	C	N	C−2s	C−2p	N−2s	N−2p
BA1−1	2.32	−0.05	−0.82	0.21	0.34	1.00	3.03	1.47	4.34
BA1−2	1.63	−0.08	−0.71	0.01	0.10	1.00	3.06	1.41	4.29
BA2−2	1.56	−1.0	−0.73	−0.02	0.07	0.98	3.09	1.40	4.32
BA3−3	1.55	−1.0	−0.77	−0.02	0.06	0.98	3.10	1.40	4.36
BA4−4	1.53	−1.0	−0.80	−0.03	0.05	0.97	3.11	1.39	4.40

[a] Electronic properties in a series of benzene−ammonia cluster ions indicating changes in the electronic structures of the C atom of benzene and the N atom of ammonia, involved in a chemical bond between them. The charges, spin densities, and atomic populations have been calculated according to the natural bond orbital (NBO) analysis, using the B3LYP/6-311+G* level of theory.

clusters of one ammonia molecule and benzene, indicating the different character of the chemical bond in these two molecules. The big difference in the bond length is also correlated with a big change of spin densities on those two atoms. According to Table 1, the spin density on carbon changes from 0.21 to 0.01 au and the spin density on nitrogen changes from 0.34 to 0.10 au. The large values of spin densities on carbon and nitrogen in the cluster BA1-1, indicates a double-radical character of the chemical bond between those two atoms. However in the BA1-2 cluster, the spin densities on both atoms are almost zero, indicating a covalent character of this chemical bond. The bond length between those two atoms becomes smaller in the series of the clusters formed by adding ammonia molecules, which is also correlated with the systematic increase of the negative value of the atomic charges on both atoms. Those changes in atomic charges indicate a systematic increase of electronic density on both atoms involved in the chemical bonding that is caused by the existence of additional ammonia molecules. The presence of additional ammonia molecules also changes the partition of electronic density between the 2s and the 2p shells of the carbon and nitrogen atoms. The 2s population of carbon becomes smaller in this clusters series, and the 2p population becomes bigger. A similar change in the atomic population is observed for the nitrogen atom. The bigger population of the 2p shell of both the carbon and the nitrogen atoms indicates a stronger character of covalent bonding between these two atoms, which decreases the length of the chemical bond between them. Therefore, our study shows how additional ammonia molecules increase the strength of the covalent bonding between two molecules in a cationic cluster, by increasing the electronic density on the atoms involved in the chemical bond.

Related effects may be observed for any chemical reaction whose products are more strongly stabilized by hydrogen bonds, and it is interesting to speculate about the *unique* features of the reaction shown in Scheme 3. The reactants and products for Scheme 3 differ by a single three-electron bond whose formation can be conveniently driven by the addition of hydrogen bond acceptor atoms. By comparison, the position of the equilibrium for a carbocation-nucleophile addition reaction (Scheme 4) might be perturbed in a similar manner by the addition of hydrogen bond acceptors. It is not clear whether the perturbation in this equilibrium would be accompanied by

SCHEME 4

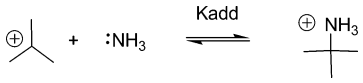

the large changes in C−N bond distance observed here for the reactions of cation radicals.

Conclusions

To summarize, we feel this paper supports three general conclusions: (1) There are two types of heterocluster ions of benzene and ammonia, a protonated form where the positive charge resides on the ammonia, and an unprotonated form where an ammonia is chemically bound to the benzene radical cation. (2) The electronic density within the $\{C_6H_6(NH_3)_{n\geq 2}\}^+$ radical cation is mainly deficient on the ammonia moiety. Positive charge can be reversibly transferred back to the benzene upon evaporation of the ammonia molecules. (3) Evidence for the most stable structure $\{C_6H_6(NH_3)_4\}^+$ was obtained both experimentally and theoretically. The stability of this "cyclohexadienyl" type complex is greatly enhanced by additional ammonia molecules hydrogen bonded to the ring-bound ammonia. These additional "solvent" ammonias appear to further strengthen the C−N bond, as their number increases.

We have investigated the expansion of benzene and ammonia via molecular beam/tandem mass spectrometry. By mass selecting cluster ions of $\{C_6H_6(NH_3)_n\}^+$, $n = 1-4$, and $\{C_6H_6(NH_3)_n\}H^+$, $n = 1-5$, we have been able to elucidate their binding features and structural differences as a function of their relative stability by using both the conventional mass spectrum and collision induced dissociation spectra. Calculations of cluster structures were carried out by density function theory at the B3LYP/6-311+G(d,p) level. The theory supports our experimental observation that the $\{C_6H_6(NH_3)_4\}^+$ ion is very stable. The structure of this cluster ion is a cyclohexadienyl radical cation with an ammonia forming a dative bond to the benzene ring, while at the same time it is solvated by three ammonia molecules, $\{C_6H_6-NH_3\}^+-\{NH_3\}_3$. As the number of solvent ammonia molecules increases, the stability of the dative benzene−ammonia bond is greatly enhanced where up to 70% of the electron density of the ammonia moiety has now been transferred to the electron deficient benzene radical cation.

Collision induced dissociation (CID) of mass selected clusters ions $\{C_6H_6(NH_3)_n\}^+$, $n = 1-4$, reveals that the electronic density is transferred back to the ammonia upon evaporation of the "solvent" ammonia molecules.

In general, one may infer from these results for benzene/ammonia, that *any* Lewis acid−base interaction should be highly solvent dependent and can be further enhanced via hydrogen bonding of the electron donor molecule by polar solvent molecules. As a result, we feel further study of the $\{C_6H_6-NH_3\}^+$ cation is warranted as a model system for solvent catalyzed aromatic cation substitution reactions. Such a model system would be able to aid in the understanding of solvent catalyzed aromatic cation substitution reactions because the solvent effect can stabilize the reaction intermediate and therefore lower the overall reaction activation energy.

Acknowledgment. J.R. wishes to acknowledge NIH grant GM39754 for support of this work. T.F. gratefully acknowledges support of NIH SBIR Grant 2R44GM065617-02. This work was performed in part at SUNY-Buffalo's Center for Computational Research.

Supporting Information Available: Structure of the benzene−ammonia complex, table of basis set superposition error (BSSE) from DFT calculations at B3LYP/6-311+G(d,p) and B3LYP/aug-cc-pVDZ level of theory, and tabulations of Mulliken charge and NBO charge distributions within cluster isomers. This material is available free of charge via the Internet at http://pubs.acs.org.

References and Notes

(1) Ussing, B. R.; Singleton, D. A. *J. Am. Chem. Soc*. **2005**, *127*, 2888.
(2) Wu, Z.; Glaser, R. *J. Am. Chem. Soc*. **2004**, *126*, 10632.
(3) Glaser, R.; Horan, C. *J. Org. Chem*. **1995**, *60*, 7518.
(4) Petrie, S.; Javahery, G.; Bohme, C. K. *J. Am. Chem. Soc*. **1992**, *114*, 9205.
(5) Mohr, M.; Marx, D.; Parrinello, M.; Zipse, H. *Chem. Eur. J*. **2000**, *6, 21*, 4009.
(6) Miyazaki, M.; Fujii, A.; Ebata, T.; Mikami, N. *Phys. Chem. Chem. Phys*. **2003**, *5*, 1137−1148.
(7) Richard, J. P.; Jagannadham, V.; Amyes, T. L.; Mishima, M.; Tsuno, Y. *J. Am. Chem. Soc*. **1994**, *116*, 6706−6712. Toteva, M. M.; Richard, J. P. *J. Am. Chem. Soc*. **1996** *118*, 11434−11445. Takeuchi, K.; Takasuka, M.; Shiba, E.; Kinoshita, T.; Okazaki, T.; Abboud, J.-L. M.; Notario, R.; Castano, O. *J. Am. Chem. Soc*. **2000**, *122*, 7351−7357. Richard, J. P.; Toteva, M. M.; Amyes, T. L. *Org. Lett*. **2001**, *3*, 2225−2228.
(8) Brutschy, B. *Chem. Rev*. **1992**, *92*, 1567; **2000**, *100*, 3891.
(9) Buchhold, K.; Reimann, B.; Djafari, S.; Barth, H.-D.; Brutschy, B.; Tarakeshwar, P.; Kim, K. S. *J. Chem. Phys*. **2000**, *112*, 1844.
(10) Riehn, C.; Lahmann, C.; Brutschy, B. *J. Phys. Chem*. **1992**, *96*, 3626.
(11) Riehn, C.; Buchhold, K.; Reimann, B.; Djafari, S.; Barth, H.-D.; Brutschy, B.; Tarakeshwar, P.; Kim, K. S. *J. Chem. Phys*. **2000**, *112*, 1170.
(12) Brenner, V.; Martrenchard-Barra, S.; Millie, P.; Dedonder-Lardeux, C.; Jouvet, C.; Solgadi, D. *J. Phys. Chem*. **1995**, *99*, 5848.
(13) Brutschy, B.; Eggert, J.; Janes, C.; Baumgartel, H. *J. Phys. Chem*. **1991**, *95*, 5041.
(14) Grover, J. R.; Cheng, B.-M.; Herron, W. J.; Coolbaugh, M. T.; Peifer, W. R.; Garvey, J. F. *J. Phys. Chem*. **1994**, *98*, 7479.
(15) Fujii, A.; Okuyama, S.; Iwasaki, A.; Maeyama, T.; Ebata, T.; Mikami, N. *Chem. Phys. Lett*. **1996**, *256*, 1.
(16) Yi, M.; Scheiner, S. *Chem. Phys. Lett*. **1996**, *262*, 567.
(17) Miyazaki, M.; Fujii, A.; Ebata, T.; Mikami, N. *Chem. Phys. Lett*. **2004**, *399*, 412.
(18) Ibrahim, Y. M.; Meot-Ner, M.; Alshraeh, E. H.; El-Shall, M. S.; Scheiner, S. *J. Am. Chem. Soc*. **2005**, *127*, 7053.
(19) Tachikawa, H. *Phys. Chem. Chem. Phys*. **2002**, *4*, 6018.
(20) Mizuse, K.; Fujii, A.; Mikami, N. *J. Phys. Chem. A* **2006**, *110*, 6387.
(21) Campargue, R. *J. Phys. Chem*. **1984**, *88*, 4466.
(22) Lyktey, M. M. Y.; DeLeon, R. L.; Shores, K. S.; Furlani, T. R.; Garvey, J. F. *J. Phys. Chem. A* **2000**, *104*, 5197 and references therein.
(23) Becke, A. D. *Phys. Rev. A* **1988**, *38*, 3098−3100.
(24) Lee, C.; Yang, W.; Parr, R. G. *Phys. Rev. B* **1988**, *37*, 785−789.
(25) Hehre, W. J.; Radom, L.; Schleyer, P. v. R.; Pople, J. A. *Ab Initio Molecular Orbital Theory*; Wiley: New York, 1986.
(26) Rablen, P. R.; Lockman, J. W.; Jorgensen, W. L. *J. Phys. Chem. A* **1998**, *102*, 3782−3797.
(27) Kong, J.; White, C. A.; Krylov, A. I.; Sherrill, C. D.; Adamson, R. D.; Furlani, T. R.; Lee, M. S.; Lee, A. M.; Gwaltney, S. R.; Adams, T. R.; Ochsenfeld, C.; Gilbert, A. T. B.; Kedziora, G. S.; Rassolov, V. A.; Maurice, D. R.; Nair, N.; Shao, Y.; Besley, N. A.; Maslen, P. E.; Dombroski, J. P.; Dachsel, H.; Zhang, W. M.; Korambath, P. P.; Baker, J.; Byrd, E. F. C.; Van Voorhis, T.; Oumi, M.; Hirata, S.; Hsu, C. P.; Ishikawa, N.; Florian, J.; Warshel, A.; Johnson, B. G.; Gill, P. M. W.; Head-Gordon, M.; Pople, J. A. *J. Comput. Chem*. **2000**, *21*, 1532.
(28) *CRC Handbook of Chemistry and Physics*, 76th ed.; Lide, D. R., Ed.; CRC Press: Boca Raton, FL, 1995.
(29) Tachikawa, H.; Igarashi, M.; Ishibashi, T. *Phys. Chem. Chem. Phys*. **2001**, *3*, 3052.
(30) Suzuki, S.; Green, P. G.; Bumgarner, R. E.; Dasgupta, S.; Goddard, W. A., III; Blake, G. A. *Science* **1992**, *257*, 942.
(31) Applegate, B. E.; Miller, T. A. *J. Chem. Phys*. **2002**, *117*, 10654.
(32) Zumdahl, S. S. *Chemistry*, 3rd ed.; D. C. Heath and Co.: Lexington, MA, 1993.
(33) Tzeng, W.; Narayanan, B. K.; Chang, G. C.; Tsai, W. C.; Ho, J. J. *J. Phys. Chem*. **1996**, *100*, 15340.